

# Long Waves Perturbations to Astronomical Tides in Adriatic and Tyrrhenian Sea

Costantino Sigismondi

*Sapienza Università di Roma and ICRA, International Center for Relativistic Astrophysics  
Piazzale Aldo Moro 5, 00185 Roma Italia email: sigismondi@icra.it*

**Abstract.** Portable tide gauges have been made with ultrasonic detectors with acquisition rate of 100 data per minute. With them we measured mean sea level variations in different locations of Adriatic and Tyrrhenian sea around latitude 42° N. Several long term variations are superimposed to astronomical tide, ranging from 4 to 60 minutes. Their nature of seiches or edge waves and their identification with transversal oscillations of the whole sea are discussed.

**Keywords:** Coastal Oceanography; Shallow Water Waves; Seiches; Tsunamis; Geophysical Instrumentation.

**PACS:** 92.10.Hm; 92.10.Sx; 92.10. Iv; 91.30. Nw; 93.

## INTRODUCTION

Averaging for some minutes continuous sea level data, we detect long waves, which are setup by wind or waves breaking and travel as shallow water waves according to sea bottom profiles.

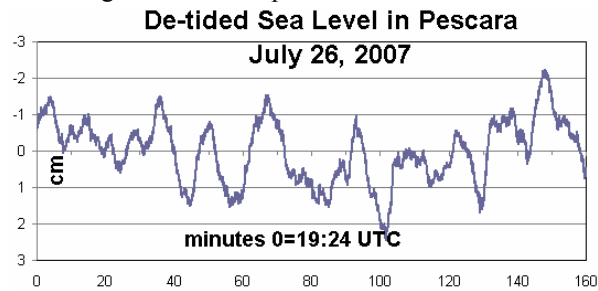


**FIGURE 1.** Sea level fluctuations. The astronomical tide is subtracted. Averages of 100 data per minute are plotted.

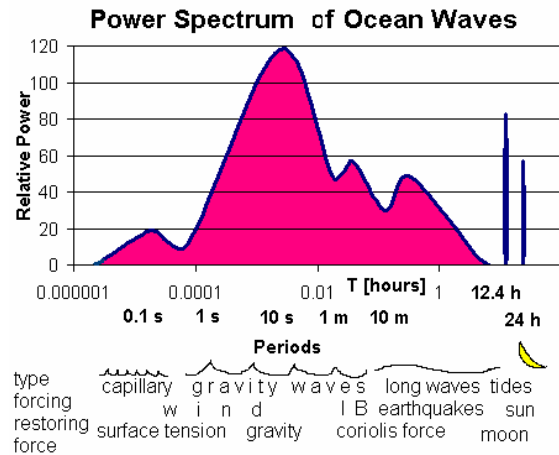


**FIGURE 2.** Relative amounts of energy as a function of wave periods in ocean waves and their classifications

based on period, wave-generating force, and restoring force. IB stands for Inverse Barometer effect.

In the Adriatic sea there are oscillations of  $T=21.2$ ; (12.5);10.8; 9.5; 8.2; 7.2 and 6.1 hours, besides diurnal and semidiurnal tides (Manca et al. 1974 in fig. 3). Shorter  $T$  appear locally in gulfs, bays and harbours.

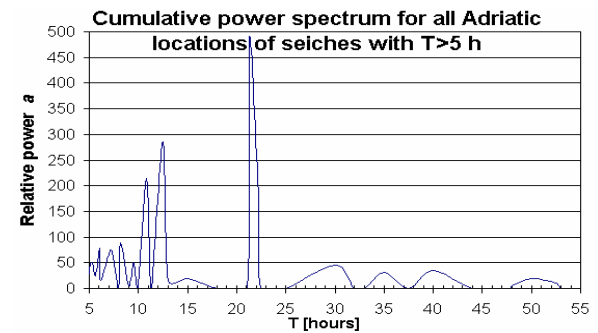


**FIGURE 3.** Spectrum has been obtained for 8 locations of Adriatic sea summing square roots of  $a^2$ , the amplitude of power spectrum for each single peak of various spectra.

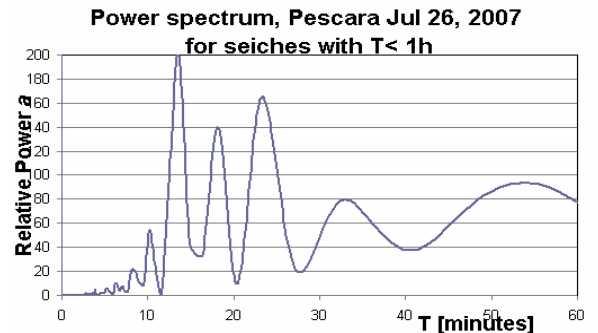


**FIGURE 4.** FFT spectrum of sea level fluctuations measured in Pescara from a pier in front of open sea, during 3 hours of calm sea conditions. Energy peaks at 11; 15; 20; 26; 36 and 60 minutes are detected.

## SHALLOW WATER WAVES

Among all kind of gravity and capillary waves, the shallow water ones, are faster for depth  $h > 1$  cm.

These are non dispersive waves, group and phase velocity are the same, depending on the square root of depth.  $v = \sqrt{gh}$ , where  $g = 9.8 \text{ m/s}^2$  and  $h$  sea depth.

This solution of wave's equation is valid when  $\lambda \geq 20h$  (Knauss, 1997). The orbits of water particles moved by the wave degenerate in horizontal oscillation to the bottom of the sea, when in shallow water regime. There frictional loss of energy occurs.

### Shallow Water Waves in Laboratory

Using a rectangular tank with about 20 cm of depth it is possible to check the square root law for the velocity of shallow water waves. Those waves are generated by lifting the tank from a side of 1-2 cm, and leaving it suddenly. The first wave is a slow transient wave and the following are fast shallow water waves preceded by small capillary waves pushed on by the main ones.

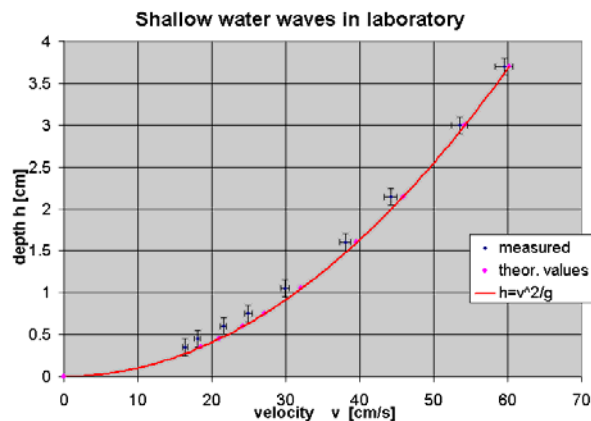


**FIGURE 5.** Shallow water waves velocity in a tank. Laboratory data compared with equation  $h = v^2/g$ .

### Waves Breaking Near Sea Shoreline

The shallow water regime rules motion and breaking of waves near the beaches. Decreasing depth waves slow down. Their wavelengths reduce but periods remain constant. Approximately when the sea depth is equal to the wave height the wave starts to break, because its trough travels  $\sqrt{2}$  slower than the crest.

### Waves Profiles

Ordinary sea waves have heights  $W \leq 1/30\lambda$  (Accordi and Palmieri, 1987); and cannot be steeper than  $W \sim 1/7\lambda$  (Bascom, 1964) for sea water viscosity. The

steepness of a wave  $s = W/\lambda$  is index of the energy present in the wave (Ricci Lucchi, 1992).

### Tides

Those waves are excited by the Moon and the Sun, their period is  $T \sim 12.4 \text{ hr} \sim 45000 \text{ s}$  (half lunar day) and their wavelength  $\lambda \sim 20000 \text{ Km}$  at the equator (half equatorial circle). Their velocity is  $v \sim 450 \text{ m/s}$ , which would require an uninterrupted ocean depth of 20 Km, for traveling as shallow water waves. Since average oceans' depth is less than 5 Km, and there are continents among them, ocean tides are much slower and they orbit around amphidromic points of zero tides, keeping their 12.4 hr main period. Evidence suggest that most tidal energy is dissipated daily in shallow seas with large tides, such as the Bering Sea and those around Great Britain and Australia (Knauss, 1997, p. 243).

This process allows energy exchange between Earth spin and lunar orbit (Goldreich, 1972) and Earth spin slows down while Moon's orbit radius enlarges gradually.

Sea level oscillations and currents are of great importance for the safety of navigation during ship maneuvers in and out of harbor. Tides are the major cause of sea level changes in the open ocean but seiches and storm surges usually play a major role in enclosed seas and lakes. The Mediterranean Sea is an example of a low-tidal region with tides up to 50 cm, except in its small shallow basins such as the Gulf of Gabes and north Adriatic Sea.

### Seiches

Standing waves with frequencies multiple of shallow water crossing time of a given basin are set up by winds and pressure disturbances. For a rectangular basin ( $a \times b$ ) and average depth  $h$  there are  $v = n\sqrt{gh}/2a$  and  $v = n\sqrt{gh}/2b$  with integer  $n = 1, 3, 5, \dots$  (Csanady, 1984).

Seiches in small harbours have 1 hour of decay time corresponding to a few periods (Yanuma and Tsuji, 1998), while the lowest-mode Adriatic seiche ( $T = 21.2 \text{ h}$ ) has a free decay time of  $3.2 \pm 0.5$  days (Cerovečki et al., 1997), corresponding to 3.6 periods. That longevity of the seiches might be related to the weak influence of bottom friction and the limited energy loss through the Otranto Strait.

### Wind setup

For wind blowing perpendicularly to the shore  $S[m] \sim V^2 f / 10^5 g h$ , where  $V$  is wind speed [m/s],  $f$  the fetch over which it blows and  $h$  average depth (Taylor expansion of 5.11 formula in Ippen, 1965). For a 100 Km fetch and  $h=100$  m, with wind at  $V=10$  m/s, near shore the sea level is 0.1 m higher.

### Wave setup

The wave setup occurs in the zone of breaking waves and the beach, and can be as much as 10 to 20 % of the incident wave height. Because of wave setup the tides are always observed higher on the beach than in a tide gauge at the end of a pier (Ippen, 1965 p. 246).

### Tsunamis

Tsunamis are low-frequency ocean waves generated by submarine earthquakes. The sudden motion of seafloor over distances of a hundred or more kilometers generates waves with periods in the range  $T \sim 10$ -60 minutes. A quick estimation shows that  $T \sim \Delta l / \sqrt{gh}$ , where  $\Delta l$  is the dimension of the source and  $h$  its depth. Their name is Japanese for “harbour wave”. They were used to estimate the depth of the Pacific ocean in 1856, when direct measurements were virtually impossible, by observing their phase speed. For North Pacific the result was 4200-4500 m, a considerable improvement on the previous estimate of 18000 m (Tomczak, 2005). Typical e-folding decay is 22 hours in open oceans (Van Dorn, 1984), and the damping is due to bottom friction and turbulence.

### Storm surge and Inverted Barometer effects

Forced oscillations of sea level – storm surges – are aperiodic changes in sea level that are mainly caused by the forcing of long-lasting and strong winds or pronounced air pressure disturbances (Proudman, 1929). Sea level theoretically adjusts to air pressure as an inverted barometer. Tsunamis can be generated also by storm surges or other pressure disturbances and they are called meteotsunami. An impulse of 1 hPa correspond to a change in local mean sea level of 1 cm, this impulse starts to propagate as shallow water wave.

### Edge Waves

Water-level changes due to proper oscillations are frequently recorded at a tide gauge station in a bay.

In the case of a tsunami, proper oscillations in the bay appear predominantly after the several initial waves. In some cases, proper oscillations are also observed at a tide gauge station located on an open coast, which suggests that standing-edge waves can be induced by meteorological disturbances on a shelf region with a straight coastline. Edge waves run parallel to the coast and have amplitudes  $\leq 5$  cm (Yanuma and Tsuji, 1998 measured them in calm days). It has been suggested that edge waves of a few centimeters amplitude are the reason that pressure gauges, which measure waves in the one- to several-minutes range, record much more energy near shore than several hundreds of meters off shore. The amplitude of these edge waves is highest at the shore and falls off rapidly seaward:  $a = a^* \exp(-kx)$ , where  $a^*$  is the amplitude at the shoreline and  $x$  the distance normal to the shore,  $k = 2\pi/\lambda$  is the wavenumber. Their velocity is  $v^2 = g \sin t/k$ ,  $v = 34$  m/s for a 15 Km long wave with the slope of the bottom  $t = 0.05$ , and  $v \sim 10$  m/s with  $t = 0.004$ .

Edge waves are produced by the variability of wave energy reaching shore. Waves tend to come in groups, especially when waves come from distant storms. For several minutes breakers may be smaller than average, then a few very large waves will break. The minute-to-minute variation in the height of breakers produces low-frequency variability in the along-shore current. This, in turn, drives a low-frequency wave attached to the beach, an edge wave. The waves have periods of a few minutes, a long-shore wave-length of a kilometer, and an amplitude that decays exponentially offshore (Stewart, 2005).

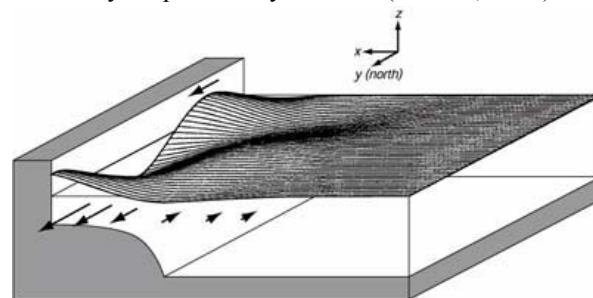


**FIGURE 6.** Edge waves exist in the breakers' zone near the beach and on the continental shelf.

Edge waves typical parameters are obtainable from shallow water equations fixing the condition that  $v^2 = g \sin t/k \leq g \langle h \rangle$   
so  $k \sim \sin t / \langle h \rangle$

and with a slope of  $\sin t \sim 10^{-3}$  and  $\langle h \rangle \sim 1$  m, averaged between breakers' zone and beach,  $k=2\pi/\lambda$  and  $\lambda \sim 6$  Km.

When sea is more agitated the depth  $h$  of breakers increases and  $\lambda$  increases linearly. For constant slope average  $\langle h \rangle = \frac{1}{2} h$  is just half of the depth at breakers' zone, and since waves break at  $h=W$ ,  $\langle h \rangle = \frac{1}{2} W$ .

$\lambda \sim 3 W$  Km, with  $W$  the average height of waves.

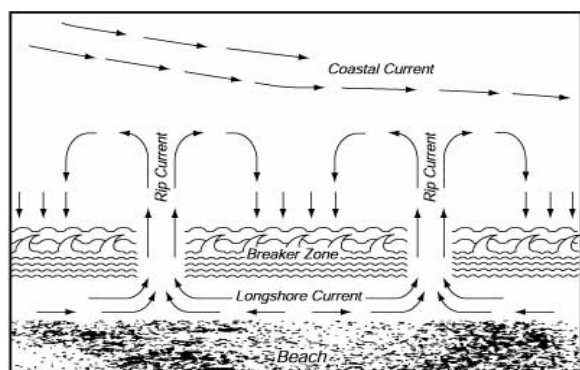


**FIGURE 7.** Rip currents generated by water carried to the beach by breaking waves. Local variations of these currents determine the onset of edge waves.

## SEICHES AND TIDAL ACTIVITY IN ADRIATIC SEA

The Adriatic Sea is a semi-enclosed sea, extending about 1000 km by 200 km and entirely surrounded by mountain chains (Appennini, Alps and Dinaric Alps). Particularly during autumn and winter, storm surge events occur in its northern part: the sea level rises to unusual values, because of the local low pressure system and of strong south-east sirocco wind channeled by orography.

If such events occur in phase with the astronomical tide, they produce the flooding of the coastal regions and the phenomenon of high water in Venice (Zampato et al., 2006). Being a semi-enclosed sea of Northern hemisphere, Adriatic sea has principal tidal waves rotating counterclockwise. They are induced by the tides of Ionian Sea and are mainly semidiurnal. Tides enter from Otranto strait and go on Eastern Adriatic up to Split, Trieste and Venice, and after pass on the Italian coast through Ancona, Pescara and Bari. The influence of principal winds on seiches activity has been studied from several authors (e.g. Polli, 1969; Manca et al., 1974; Vilibić and

Mihanović, 2003). when a cyclone approaches the Adriatic, the sea level rises in its northern part due to the combined action of the low air pressure and Sirocco wind; after the cyclone and its frontal system have left the area, the air pressure increases and the wind suddenly slackens or even changes direction to Bora, which triggers the seiches (Belušić et al. 2007). The principal seiche has a period of 21.2 h and is a longitudinal oscillation of the whole sea from SE to NW, excited by the Sirocco wind. In the Adriatic Sea the southeast winds (Sirocco) raise the sea level, especially in the North Adriatic, where a long-lasting Sirocco and low air pressure can raise the water level up to 1 m. Wind influence is less important in the South Adriatic, where the air pressure influence is dominant giving rise to sea level changes of up to 30 cm (Vilibić, 2005). Spreading of tides in the Adriatic is usually described by the largest M2 (Principal lunar semidiurnal  $T=12$  h 25 m) and K1 (Lunisolar diurnal  $T=23$  h 56 m) with P1 (Principal solar diurnal  $T=24$  h 04 m) constituents (Fig. 8, adapted after Polli, 1960) while other semidiurnal and diurnal constituents behave similarly to M2 and K1, respectively. Their amplitudes are higher than in the rest of the Mediterranean, especially in the northern Adriatic, primarily due to near-resonant coupling of the equilibrium tide with the Adriatic topography through the co-oscillation with the Ionian and Eastern Mediterranean tides. A common characteristic of the semidiurnal tides is rotation around the amphidromic point that is positioned between Ancona and Šibenik (Sebenico in fig. 8), having small amplitudes there. The amplitudes increase rapidly from that point to the northwest, with the maximum values inside the Gulf of Trieste (M2 tide amplitude equals 26 cm). Semidiurnal amplitudes also increase from the amphidromic point to the southeast, reaching the maximum between Pelješac peninsula and Italian coast, but their values are less than half of the maximum ones occurring in the North Adriatic. Diurnal tides propagate from the Croatian to the Italian coast, whereas the amplitudes increase from the South to the North Adriatic. K1 amplitude varies from 5 cm at Dubrovnik (Ragusa in fig. 8) to 18 cm in the Gulf of Trieste. Relative amplitudes of different tides are  $M2=100$ ;  $K1=58.4$  and  $P1=19.4$  (Knauss, 1997). In front of Pescara K1 and P1 cross Adriatic in about  $24^\circ$ , i.e. in 1 h 36 m or 96 minutes.



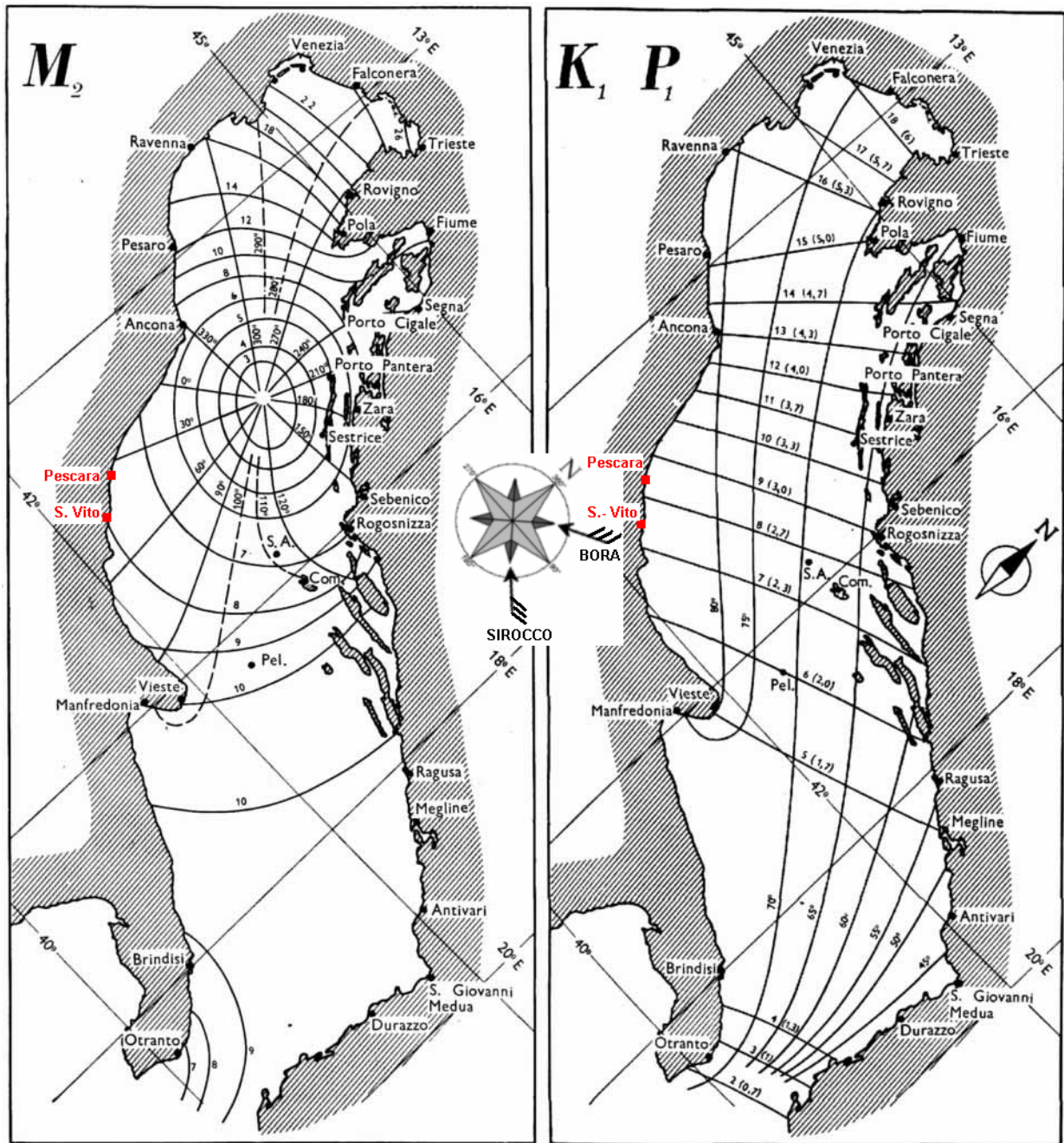


**FIGURE 8.** The spreading of major semi-diurnal  $M_2$  and diurnal  $K_1$  and  $P_1$  (between parentheses) tides in the Adriatic Sea. All measured in cm. Their phase is expressed in degrees. From Ancona to Vieste in Italian coast, the western boundary of Adriatic basin, the  $K_1$  and  $P_1$  wave individuate a very large bay of 287 Km of width, and Pescara and S. Vito are located at its centre. The presence of Mid Adriatic Pit at -266 m, just in front of Pescara, should update this figure with a slight bending South-westward of the 80° phase line. On the pit the tidal wave propagate faster than over shallower sea floor. The principal winds are also shown: Bora blowing from North East and Sirocco from South East. The phase angle 0° of  $M_2$  component corresponds to 0° of  $K_1$  and  $P_1$  only at syzyzy, when Sun and Moon transit at (anti) meridian at the same time (Tenani, 1940).

## LONG WAVES DETECTION

Mobile tide gauges made with ultrasonic range finders have been implemented to study the propagation of long waves in coastal sea.

The detector chosen for those measurements is the ultrasonic range finder sensor SRF02 ([www.robot-electronics.co.uk/htm/srf02techI2C.htm](http://www.robot-electronics.co.uk/htm/srf02techI2C.htm) for technical specifications) with an interface board chip FTDI FT 232 R USB ([www.Ftdichip.com](http://www.Ftdichip.com) for driver and documents related). The operative range is 15 cm – 6 m, it works at tension of 5 V with currents of 4 mA producing impulses at 40 KHz with little energy consume for laptop computer. We obtained 3 hours of continuous operating time data on sea.

The original software USB\_I2C\_SRF08.exe belongs to Microsoft Foundation Classes Library and the source is public. We made it able to record data files. Distances from the detector to the water surface are sampled 100 times per minute.

From laboratory tests the detector has an angular field of view of  $38^\circ$ , and detects reflected impulses from flat surfaces with tilt angles  $\leq 27^\circ$ .

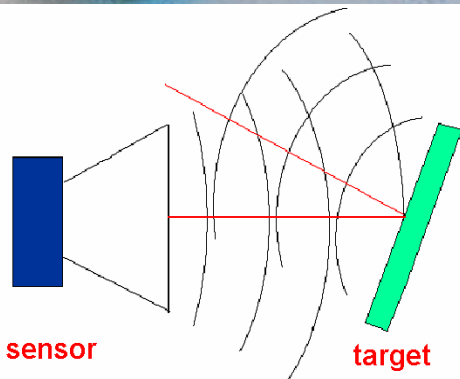
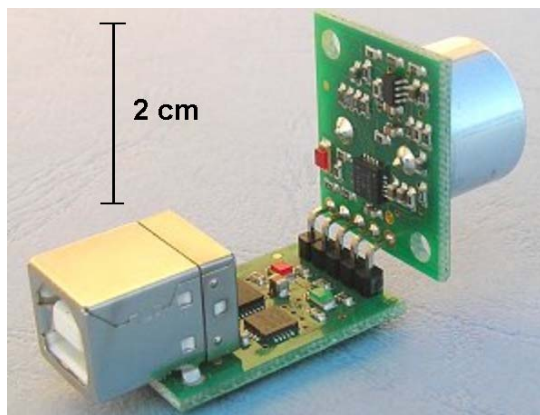


FIGURE 9. The SRF02 transducer and its field of view.

When used on the sea surface, the detectors have to be fixed on wooden arms, for their temperature stability. Better measurements are obtained in calm sea and no-wind conditions, or at least in small basins ( $\sim 1 \text{ m}^2$ ) in communication with open sea. When larger waves are passing the tilt angle of water surface produce spurious data with zeros or multiple reflection readings. They have been rejected in data analysis. To synchronize observations for measuring the velocity of seiches, time control has been made either via internal computer clock and via UTC synchronized watch. Shadowed points on piers were the most suitable locations for these measurements.

Finally two detectors working within 2 m simultaneously create interferences with spurious beats of 6 min for SRF02 version 3 (or less than 2 min scale for version 4) with amplitudes up to 35(20) cm, also average sampling rate varies within 2%.

In data analysis the running average over 1 minute and more allowed to eliminate the effect of faster wave motions. National Marine Service data have 1 h rate (APAT RMN see Tirozzi et al., 2005) and have been used as tidal trend check.

## DATA AND DISCUSSION

The measurement of velocity of long waves from offshore on the pier of San Vito (Adriatic sea, figs. 10 and 11) shows a velocity much slower than that of shallow water waves. Probably because of combined effect of fresh water input of nearby (40 m) Feltrino river and submarine barriers. In Ostia (Tyrrhenian sea) the long waves arrive simultaneously on shore at 500 m of distance as if their wavefront is parallel to the shore as seiches (fig. 12). Tyrrhenian seiches range from 20 to 40 minutes (fig. 12 and 13), slightly longer than Adriatic ones (fig. 1 and 10). There is much noise (energy at short periods) during storm than in calm sea and on-shore than off shore because of turbulence induced by wave breaking.

In deep sea a seiche of  $T=26$  min (fig. 4) has a length of  $\lambda=78$  Km in Adriatic ( $h\sim 250$  m width  $w=175$  Km  $w/\lambda\sim 2.2$ ) and one of  $T=41$  min (fig. 14) has  $\lambda=230$  Km in Tyrrhenian sea ( $h\sim 900$  m from Ostia to Sardinia  $w=245$  Km,  $w/\lambda\sim 1$ ). Integer ratios  $w/\lambda$  suggest that those seiches are transversal basin's resonances.

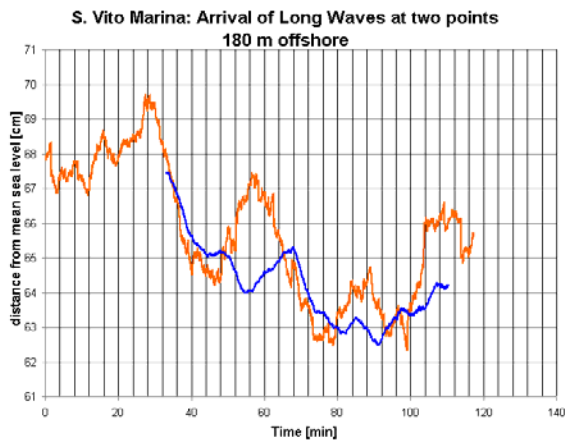


**FIGURE 10.** Adriatic Sea, pier of S. Vito Marina. Velocity experiment perpendicularly to the shore. Data of September 4, 2007 from 7:30 to 9:30 UTC with very calm sea conditions. Running averages over 10 minutes (shore, the longer line drawn) and 6 minutes (end pier, 180 m offshore, the shorter line drawn). We detected smaller amplitude waves for the position located 180 m offshore. Different patterns. Possible anti-phase between the simultaneous tracks, with a node located between the two observers; or combination of direct, incoming from offshore, and reflected waves (see following figure).

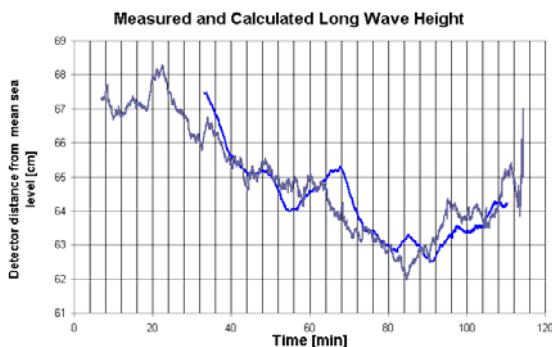


**FIGURE 11.** Adriatic Sea, pier of S. Vito Marina. Velocity experiment perpendicularly to the shore. Measured (blue and shorter track) and calculated (longer line) long wave heights. From data of September 4, 2007 the calculated height is obtained from the near-shore mean sea level record (the longer one in fig. 6) with the equation  $H_{off}(t) = [H_{on}(t-\tau) + H_{on}(t+\tau)]/2$ .

In the position offshore (180 m) the wave going to the shore at time  $t$  is  $H_{on}(t+\tau)$ , because it will arrive at shore after crossing the 180 m in  $\tau$  minutes. In the same position the wave reflected from (on)shore is  $H_{on}(t-\tau)$  which left the shore  $\tau$  minutes before arriving at the position offshore. For  $\tau = 7$  minutes we found the calculated profile closer to the measured curve. This value implies a propagation velocity of  $v=0.43$  m/s, which in shallow water regime implies a 1.9 cm

depth. Such a shallow water can be a layer of fresh water come from nearby Rio Feltrino river.

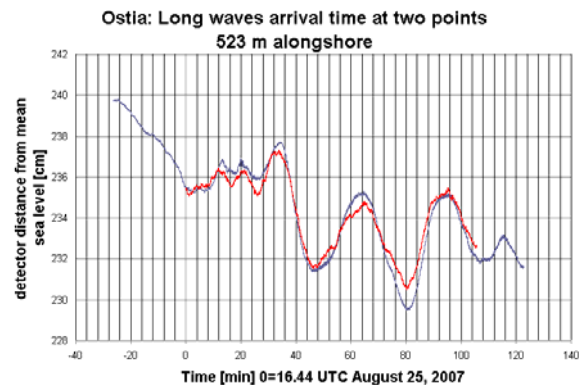


**FIGURE 12.** Velocity experiment along shore (Lido di Ostia, Tyrrhenian sea). Data of August, 25 2007. Two observers located at 523 m of relative North East (red) - South West (blue-longer duration) distance, both at 10 m offshore. Such waves seems to have same phase and slightly smaller amplitude for NE location than SW. Those data suggest a wave front parallel to the shore.



**FIGURE 13.** Data obtained during a sea storm 100 m inside the fishermen's canal-port of Ostia (Tyrrhenian sea). 4 minutes edge waves disturbances are visible superimposed to main seiches of 30-40 minutes periods. Open sea waves of 2 m height were measured during that storm. Running average on 8 minutes and tidal trend averaged on 25 minutes subtracted; other combinations of averages show similar patterns. Waves direction was from SW, and the canal is oriented toward South. The canal depth is  $h=1.4$  m and its width 15 m. With wavelengths  $\lambda=21.7 \pm 0.9$  m and periods of  $6.7 \pm 0.9$  s the waves, in this canal, propagate in shallow water regime at a speed  $v=3.24 \pm 0.57$  m/s. Shallow water speed for this canal is  $v=\sqrt{gh}=3.70$  m/s. The effect of wave setup which modulates the 20 to 40 minutes seiches with 4 minutes fluctuations is efficient even inside the canal.



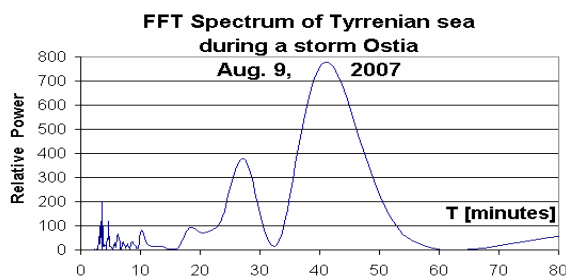


**FIGURE 14.** FFT spectrum of sea level fluctuations measured in Ostia, fishermen's canal during 3 hours of sea storm with 2 m waves (data in fig. 13). Energy peaks at 3.6; 4.6; 6.3; 10.2; 18.2; 27.3 and 41 minutes are detected.

### ACKNOWLEDGMENTS

Thanks to Prof. Giovanni Bernardini for having realized the idea of portable tide gauge proposing and using ultrasonic detector. I want to thank also Ing. Giorgio Sordello, former director of Alessandro Volta Institute in Rome, who first encouraged and financed these experiments. Thanks to Prof. Remo Ruffini and thanks to Ing. Marco Buccione for his technical support in ICRANet. Thanks to my father Camillo Sigismondi, who helped me in the observational campaign in Adriatic sea, and to my students for the Tyrrenian sea.

### REFERENCES

1. Accordi, B. and E. Lupia Palmieri, *Il Globo Terrestre e la sua Evoluzione*, Zanichelli, Bologna, Italy (1987).
2. Bascom, W. *Beaches and Waves*, Anchor Book Doubleday NY (1964).
3. Belušić, D. et al., *Resonantly Coupled Devastating Air-Sea Event in The East Adriatic: The Atmospheric Component*, proc. of VII Conference on Coastal Atmospheric and Oceanic Prediction and Processes-American Meteorological Society (2007).
4. Cerovečki, I., M. Orlić, and M.C. Hendershott, *Adriatic seiche decay and energy loss to the Mediterranean*. Deep-Sea Research I, **44**: 2007-2029 (1997).
5. Caputo, M. and G. Faita, *Primo Catalogo dei Maremoti delle Coste Italiane*, Accademia Nazionale dei Lincei, Roma (2000).
6. Csanady, G. T., *Circulation in the Coastal Ocean*, Reidel Pub. Co., Dordrecht, Holland (1984).
7. Goldreich P., *Tides and Earth-Moon System*, Scientific American, **226**, 42-52 (1972).
8. Ippen, A., *Estuary and Coastline Hydrodynamics*, McGraw-Hill, Tokyo (1966).
9. Knauss, J. A., *Introduction to Physical Oceanography*, Prentice Hall, NJ (1997).
10. Manca, B., F. Mosetti, and P. Zennaro, *Analisi spettrale delle sesse dell'Adriatico*, Boll. Geofis. Teor. Appl., **16**, 51-60 (1974).
11. Polli, S., *La Propagazione delle Maree nell' Adriatico*, Atti del IX Convegno dell'Associazione Geofisica Italiana, Roma, 1-11 (1960).
12. Polli, S., *Effetti Meteorici, Statici e Dinamici sul Livello dell'Adriatico Settentrionale*, Istituto Sperimentale Talassografico, Trieste (1969).
13. Proudman, J., *The effects on the sea of changes in atmospheric pressure*, Geophysical Supplement to the Monthly Notices of the Royal Astronomical Society, **2(4)**, 197-209 (1929).
14. Pugh, D., *Changing Sea Levels*, Cambridge University Press, Cambridge (2004).
15. Ricci Lucchi, F. *I Ritmi del Mare, sedimenti e dinamica delle acque*, La Nuova Italia Scientifica, Roma (1992).
16. Stewart, R. H., *Introduction to Physical Oceanography*, [http://oceanworld.tamu.edu/resources/ocng\\_textbook/](http://oceanworld.tamu.edu/resources/ocng_textbook/) (2005).
17. Tenani, M., *Maree e Correnti di Marea*, Istituto Idrografico della Marina, Genova (1940).
18. Tirozzi, B. et al., *Neural Networks and Sea Time Series*, Birkhäuser, Boston (2005).
19. Tomczak, M., *An Introduction to Physical Oceanography*, [ww.es.flinders.edu.au/~mattom/IntroOc/newstart.html](http://ww.es.flinders.edu.au/~mattom/IntroOc/newstart.html) (2005).
20. Van Dorn, W. G., *Some Tsunami Characteristics Deducible from Tide Records*, J. Phys. Ocean. **13**, 353-363 (1984).
21. Vilibić, I. and H. Mihanović, *Resonance in Ploče Harbor (Adriatic Sea)*, Acta Adriatica, **46**, 125-136 (2005).
22. Vilibić, I., et al., *A new approach to sea level observations in Croatia*, GEOFIZIKA, **22**, 21-57 (2005).
23. Yanuma, T. and Y. Tsuji, *Observation of Edge Waves in the Vicinity of Makurazaki Shelf*, J. of Oceanography, **54**, 9-18 (1998).
24. Zampato, L., G. Umgiesser, and S. Zecchetto, *Storm surge in the Adriatic Sea: observational and numerical diagnosis of an extreme event*, Advances in Geosciences, **7**, 371-378, (2006).